

## Surface Morphology Variation of Pt-Al<sub>2</sub>O<sub>3</sub> Thin Catalyst Films

Jae-Suk Lee, Sang-Mo Shin<sup>1</sup> and Jong-Wan Park

Dept. of Metallurgical Engineering, Hanyang University, Seoul 133-791, Korea

<sup>1</sup>Korea Electronics Technology Institute, 455-6 Jinwi, Pyungtaek, Kyunggi 451-850, Korea

(Received July 4, 1995; accepted August 26, 1996)

**Key words:** Pt catalyst, surface morphology, micro gas sensor

Platinum is one of the most versatile, all-purpose heterogeneous metal catalysts and Al<sub>2</sub>O<sub>3</sub> is also one of the best supporting materials. In this study, the surface morphology variation of Pt-Al<sub>2</sub>O<sub>3</sub> films was investigated. The attainment of a large surface area and a large fraction of high index planes (hkl) are among the most important influences on the properties of a catalyst. Scanning electron microscope (SEM) and atomic force microscope (AFM) observations revealed that Pt films deposited on Al/SiO<sub>2</sub>/Si substrates followed by thermal oxidation had relatively high surface areas in comparison to Pt films deposited on Al<sub>2</sub>O<sub>3</sub>/SiO<sub>2</sub>/Si substrates and subsequently annealed. It was proved through selected area diffraction (SAD) and X-ray diffraction (XRD) analyses that the films were composed of Pt metal and Al<sub>2</sub>O<sub>3</sub> instead of Pt-Al or Pt-Al-O compounds. The results of this study can be applied to the development of micro gas detection devices such as a micromachined catalytic thin film gas sensor with high sensitivity.

### 1. Introduction

Heated Pt coil has been used as a combustible gas sensor for a long time due to its outstanding catalytic behavior. However, evaporation of the Pt coil itself due to high temperature operation was a serious problem with regard to long-term stability. In 1962, Baker developed a new type of catalytic gas sensor known as a 'pellistor' which was composed of Pt coil as a heater, Al<sub>2</sub>O<sub>3</sub> bead as a supporting material, and a noble metal catalyst as a sensing component.<sup>(1)</sup> As an alternative to the pellistor, catalytic combustible Si micro gas sensors have been investigated by many researchers using micromachining and thin film deposition techniques<sup>(2-7)</sup> due to their low power consumption, excellent reproducibility, possibility of integration, and low cost fabrication. To acquire high

sensitivity, catalysts with a large fraction of dissociative adsorption multiplets, heaters with a high temperature coefficient of resistance (TCR), and sensor assemblies with good thermal isolation are important factors in the fabrication of catalytic combustible micro gas sensors. Of these, the fraction of dissociative adsorption multiplets of the catalyst is of prime importance. Despite its importance, the dissociative adsorption multiplets of noble metal catalysts for thin film devices have seldom been studied systematically.<sup>(8-11)</sup> In order to obtain high gas sensitivity, catalysts for a micro gas sensor should have as many dissociative adsorption multiplets as possible, which can be provided by a large surface area and a large fraction of high index planes. This requirement can be met by the new method investigated in this study.

## 2. Experiments

P-type (100) Si wafers were cleaned using the RCA process. First, in order to investigate the effect of Pt thickness variation, a 400-Å-thick Al oxide was grown by the wet oxidation process, then 600-Å-thick Al films were deposited by thermal evaporation and Pt films with different thicknesses were subsequently deposited by E-beam evaporation. The substrate temperature was 100°C (specimen A). Second, in order to investigate the effect of SiO<sub>2</sub> as a diffusion barrier, thermal oxides were grown with different thicknesses and Pt/Al films were subsequently deposited by the same method with a fixed Pt thickness of 180 Å (specimen B). Third, for comparison, a 400-Å-thick thermal oxide was grown by the wet oxidation process, then Al<sub>2</sub>O<sub>3</sub> films were prepared by either reactive sputtering of Al in Ar + O<sub>2</sub> atmosphere (300 W, 5 mTorr, O<sub>2</sub>:Ar = 1:1) or thermal oxidation of the evaporated Al (600°C, 30 min, wet O<sub>2</sub>, 0.5 l/min) and Pt/Al films were subsequently deposited in the same way as for specimen B (specimen C). The deposited films were annealed in a wet oxygen atmosphere in a tube furnace at 600°C for 30 min. The multilayer structures of the specimens prepared are shown in Fig. 1. The surface morphology of the

Pt 120, 150, 180 Å	Pt 180 Å	Pt 180 Å
Al 600 Å	Al 600 Å	Al <sub>2</sub> O <sub>3</sub> 500 Å
SiO <sub>2</sub> 400 Å	SiO <sub>2</sub> 0, 100, 200 Å	SiO <sub>2</sub> 400 Å
p-Si(100)	p-Si(100)	p-Si(100)
specimen A	specimen B	specimen C

Fig. 1. Specimen classifications

as-deposited and the wet oxidized films was observed by scanning electron microscopy (SEM) and atomic force microscopy (AFM). The crystal structures of these films were investigated by low angle X-ray diffraction (XRD) with Ni filtered Cu  $K_{\alpha}$  radiation and selected area diffraction (SAD) of transmission electron microscopy (TEM) at 200 kV.

### 3. Results

#### 3.1 Specimen A

Figure 2 shows Gibbs free energies of formation of  $\text{Al}_2\text{O}_3$ ,  $\text{Al}_2\text{SiO}_5$ ,  $\text{Al}_6\text{Si}_2\text{O}_{13}$ ,  $\text{SiO}_2$ , and  $\text{PtO}_2$ .<sup>(12)</sup> The formation energy of  $\text{Al}_2\text{O}_3$  is negative throughout the temperature range from room temperature to 2,000°C, and while that of  $\text{PtO}_2$  is positive, Al in the Pt/Al films can be preferentially transformed to  $\text{Al}_2\text{O}_3$ . Therefore, there is no tendency towards transformation of Pt metal to  $\text{PtO}_2$ , particularly in the presence of easily oxidizable metals such as Al. From the thermodynamic point of view, Pt/Al films will be oxidized to form Pt- $\text{Al}_2\text{O}_3$  during the wet oxidation process. SEM secondary electron and energy dispersive spectroscopy (EDS) mapping images with Pt windows of the as-deposited and wet oxidized films are shown in Fig. 3. Before oxidation, the films had a flat and smooth surface morphology

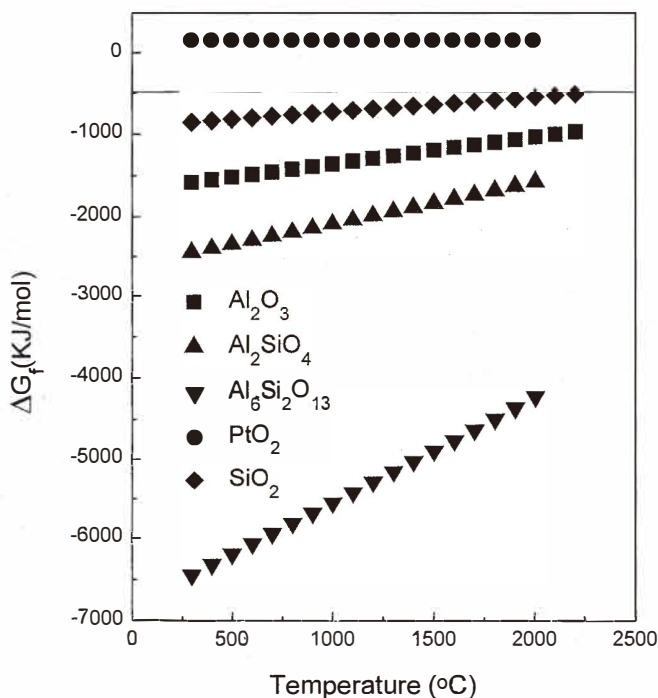


Fig. 2. Gibbs free energies of formation of  $\text{Al}_2\text{O}_3$ ,  $\text{Al}_2\text{SiO}_5$ ,  $\text{Al}_6\text{Si}_2\text{O}_{13}$ ,  $\text{SiO}_2$ , and  $\text{PtO}_2$ .

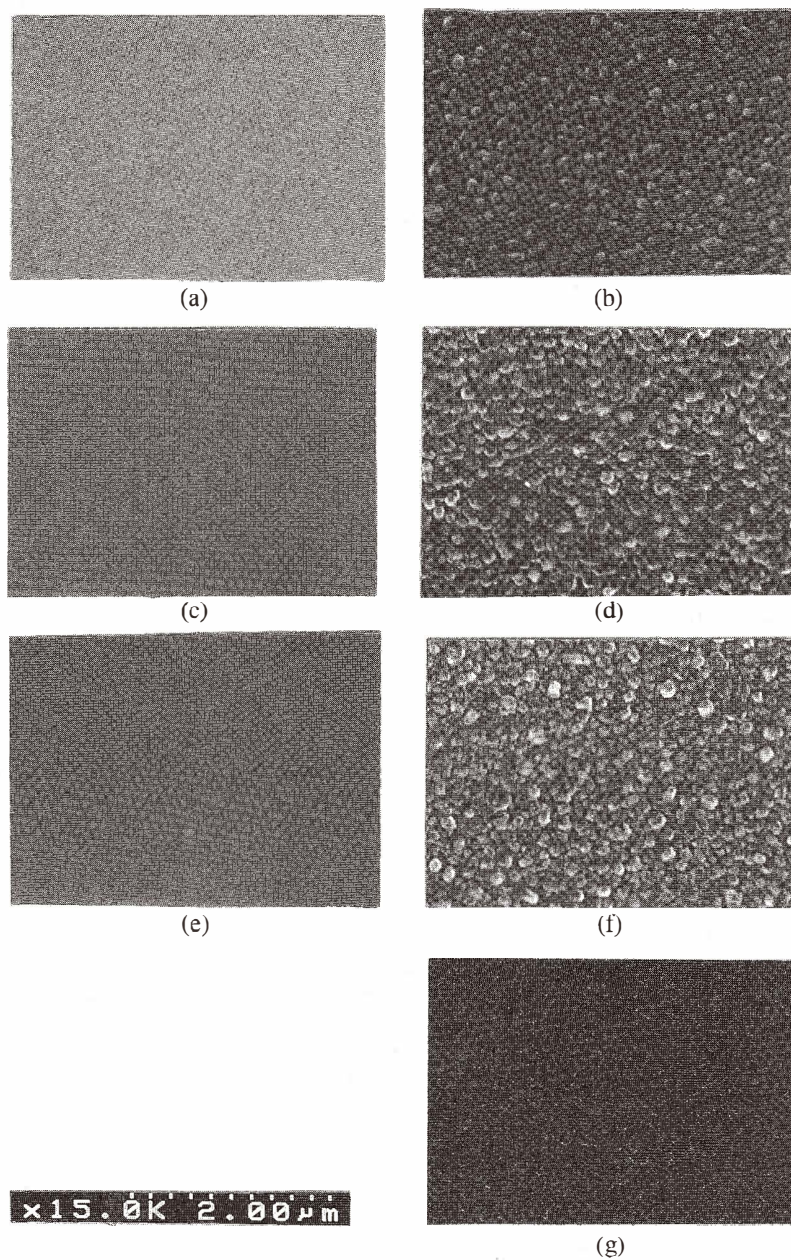


Fig. 3. SEM micrographs of specimen A; (a) as-deposited Pt (120 Å), (b) wet oxidized at 600°C for 30 min of (a), (c) as-deposited Pt (150 Å), (d) wet oxidized at 600 Å for 30 min of (c), (e) as-deposited Pt (180 Å), (f) wet oxidized at 600°C for 30 min of (e), and (g) EDS mapping of (b).

but after oxidation, from the EDS mapping, it was confirmed that the Pt films were agglomerated in the form of small buttons or beads ranging from 100–2,000 Å in size. As the Pt thickness increased, the surface roughness and, in turn, the surface area also increased. The size of the agglomerates does not appear to change. It was thought that the Pt agglomeration in the specimens depended not only on the high wetting angle between aluminum oxide and platinum films, but also on the breakdown of the Pt films due to Al oxidation by oxygen diffusion through the Pt films. Therefore, the driving force for Pt agglomeration was characterized by two factors; surface energy decrease and Al oxidation. AFM images of Pt/Al films are shown in Fig. 4. The as-deposited films had a smooth surface but the surface roughness increased after oxidation. Such increases in the surface area were confirmed by cross-sectional TEM. As shown in Fig. 5, the as-deposited Pt/Al

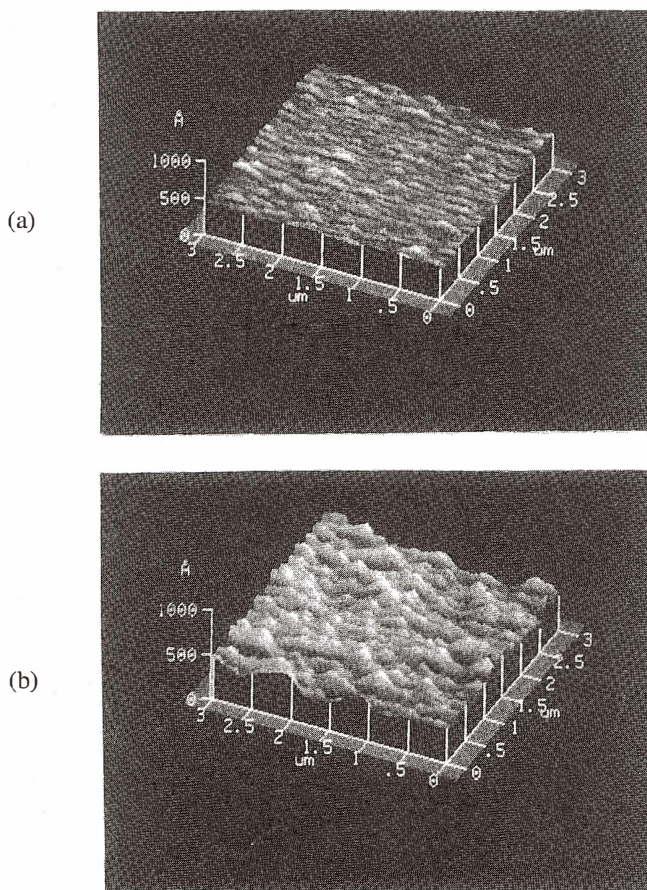


Fig. 4. AFM images of specimen A; (a) as deposited Pt (180 Å) and (b) wet oxidized at 600°C for 30 min of (a).

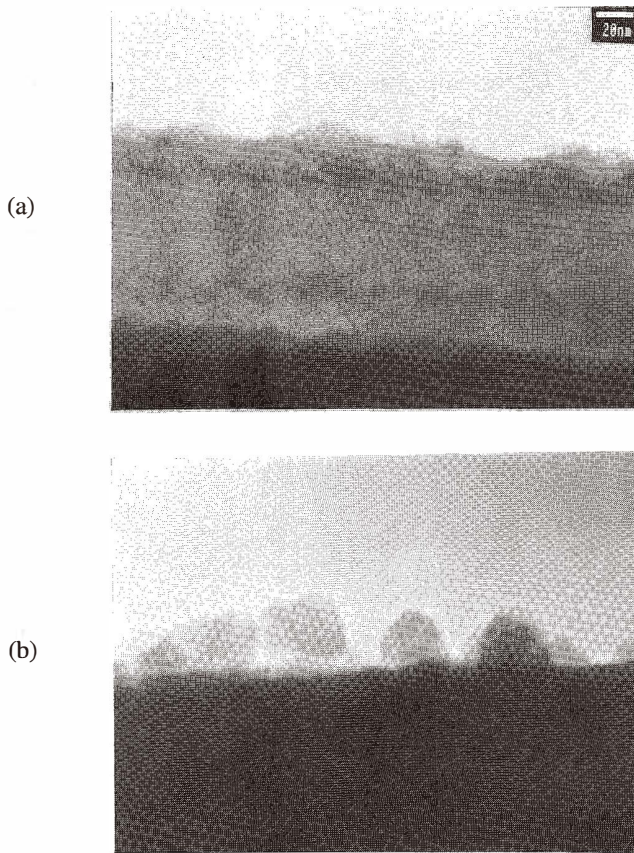


Fig. 5. Cross-sectional TEM bright-field micrographs of specimen A; (a) as-deposited Pt (180 Å)/Al (600 Å) and (b) wet oxidized at 600°C for 30 min of (a).

films changed from their initial planar form to island form during wet oxidation. In order to characterize the structure of the agglomerated films, SAD analysis of XTEM was carried out for the metallic Pt phase, the Pt-Al compound, or the Pt-Al-O compound structure. However, the agglomerated films were too thin for identification of the structure. Therefore, the top-view TEM specimens were prepared for SAD observation. The SAD patterns in Fig. 6 show that the as-deposited and the agglomerated films have an identical metallic Pt phase of fcc structure and it was confirmed that the agglomerated films are Pt and not Al which has the same fcc structure. The low angle ( $3^\circ$ ) XRD patterns of the oxidized Pt/Al film are shown in Fig. 7. Only peaks of  $\alpha$ - $\text{Al}_2\text{O}_3$  and Pt can be observed. The SAD and XRD analyses showed that the Al/Pt films were oxidized to form Pt- $\text{Al}_2\text{O}_3$  without the formation of Al-Pt compounds such as cubic  $\text{Al}_2\text{Pt}$ , tetragonal  $\text{AlPt}_3$ ,  $\text{Pt}_8\text{Al}_{21}$ , orthorhombic

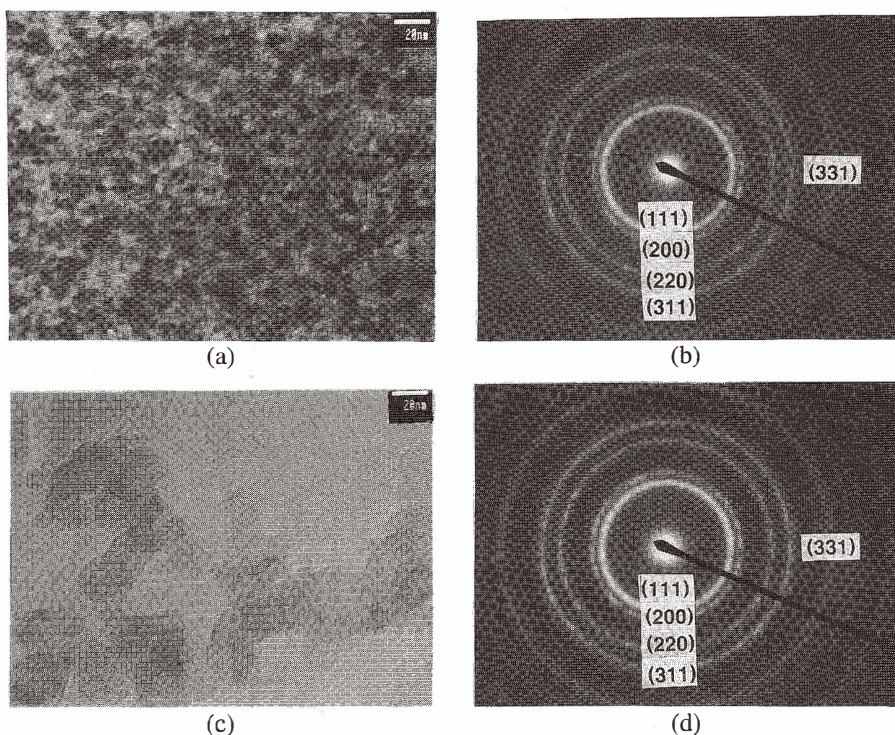


Fig. 6. Top-view TEM bright-field micrographs and SAD patterns of specimen A: (a) as-deposited Pt(180 Å), (b) SAD pattern of (a), (c) wet oxidized at 600°C for 30 min of (a), and (d) SAD pattern of (c).

Pt<sub>2</sub>Al, hexagonal Al<sub>21</sub>Pt<sub>6</sub> and Al-Pt-O ternary compounds. Therefore, it was thought that Al oxidation is more favorable than formation of any Al-Pt compound.

### 3.2 Specimen B

The specimens with relatively thin or no SiO<sub>2</sub> barriers seem to have very different surface morphology features compared to those of specimen A. In Fig. 8, SEM and EDS mapping images of the wet oxidized films are shown. Probably due to the fact that Si can diffuse into Al very easily, the surfaces of the films contain features resembling a combination of hills and valleys or bumps. The surface roughness seems to change as a function of SiO<sub>2</sub> barrier thickness. The microstructural changes of the oxidized films may be considered to be complex Al-Si-O ternary compounds or well known aluminum silicates such as orthorhombic andalusite (Al<sub>2</sub>SiO<sub>5</sub>), sillimanite (Al<sub>2</sub>SiO<sub>5</sub>), mullite (Al<sub>6</sub>Si<sub>2</sub>O<sub>13</sub>) and triclinic kyanite (Al<sub>2</sub>SiO<sub>5</sub>), since the Gibbs formation free energies of these compounds are lower than Al<sub>2</sub>O<sub>3</sub> or SiO<sub>2</sub> as shown in Fig. 2. However, the above speculation was not confirmed in this study. EDS mapping proved that the rectangular grains in the films were

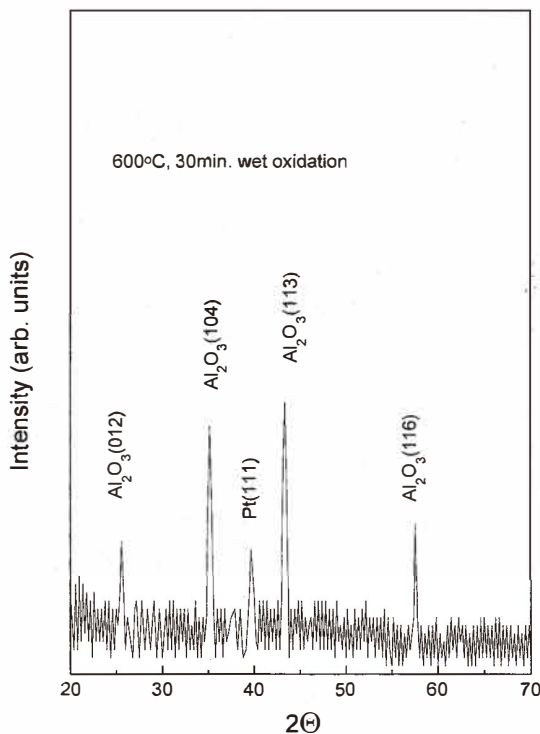


Fig. 7. XRD pattern of the wet oxidized Pt (180 Å)/Al (600 Å) film at 600°C for 30 min of specimen A.

metallic and facet phases were formed. However, this method did not provide a larger Pt catalyst surface area than that of specimen A. Because Pt films have low index plane facet features, the number of dissociative adsorption multiplets, which is one of the most important factors for catalyst sensitivity, might be lower than that of specimen A.

### 3.3 Specimen C

Specimen C was prepared using the general method for forming Pt film catalysts. SEM secondary electron and EDS mapping images of Pt films deposited on thermally oxidized and reactively sputtered Al<sub>2</sub>O<sub>3</sub> films are shown in Fig. 9. The Pt films show no sign of agglomeration after annealing in the oxygen atmosphere at 600°C but do show some features in the form of big islands after annealing at 800°C. Since the relatively thick and flat surface did not provide a large surface area, agglomeration took place at a higher temperature than in specimens A and B. EDS mapping confirmed that the agglomerated films are Pt. The agglomerated films have high index planes; however, they have relatively small surface coverage. Therefore, this method did not yield better results than the specimen A in terms of large Pt catalyst surface areas.

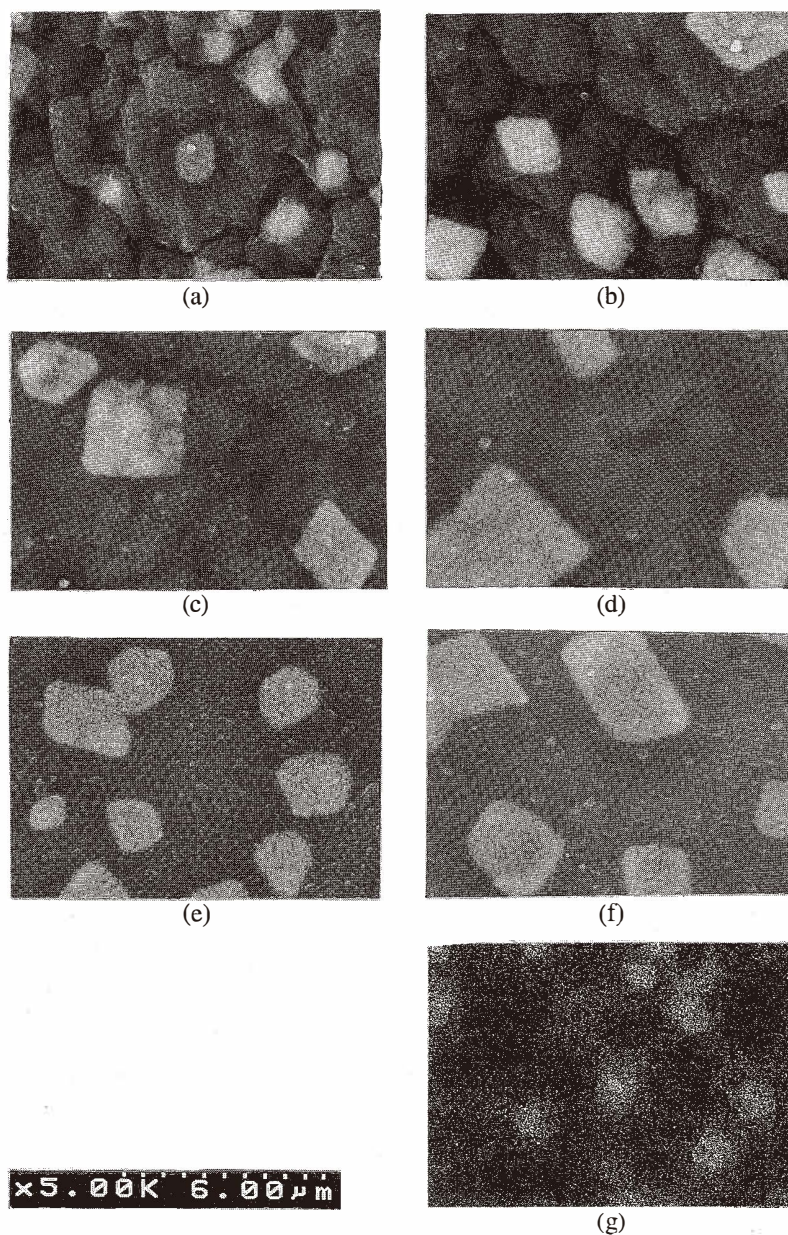


Fig. 8. SEM micrographs of the wet oxidized Pt (180 Å)/Al (600 Å) films for 30 min of specimen B; (a) at 500°C with no SiO<sub>2</sub> barrier, (b) at 600°C with no SiO<sub>2</sub> barrier, (c) at 500°C with SiO<sub>2</sub> (100 Å) barrier, (d) at 600°C with SiO<sub>2</sub> (100 Å) barrier, (e) at 500°C with SiO<sub>2</sub> (200 Å) barrier, (f) at 600°C with SiO<sub>2</sub> (200 Å) barrier, and (g) EDS mapping of (a).

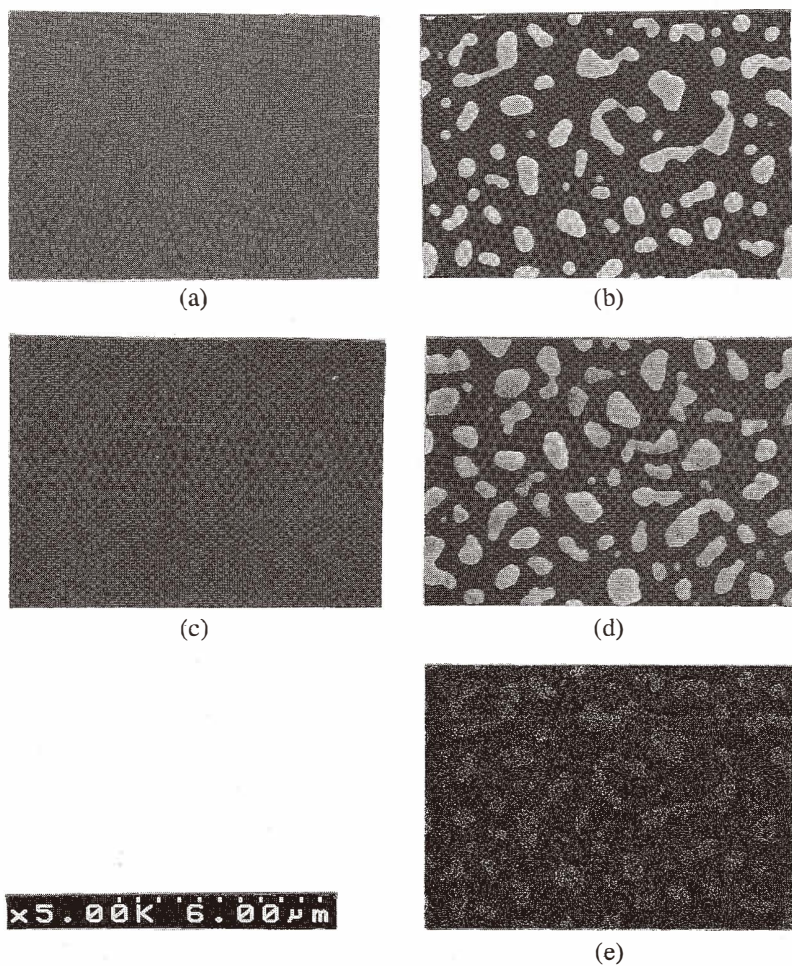


Fig. 9. SEM and EDS mapping micrographs of specimen C; (a) as-deposited Pt films on wet oxidized  $Al_2O_3(500^\circ C)$ , (b) annealed at  $800^\circ C$  for 30 min in wet  $O_2$  atmosphere of (a), (c) as-deposited Pt films on reactively sputtered  $Al_2O_3(500^\circ C)$ , (d) annealed at  $800^\circ C$  for 30 min in wet  $O_2$  atmosphere of (c), and (e) EDS mapping of (b).

#### 4. Discussion

The rate of catalytic reaction on the Pt surface depends on the number of dissociative adsorption multiplets in terms of surface area and surface plane index. Therefore, steps and kinks are very important for the catalytic behavior since adsorption and dissociation are more easily achieved at steps and kinks than at terraces. However, the sensitivity of low

index planes such as Pt(111) surfaces is an order of magnitude lower than high index planes such as Pt(557) and (679). Pt(557) has a stable surface structure with 18% of the surface atoms in monoatomic height steps and Pt(679) has, in addition to the high step density, a high density of kinks in the step or atoms of lower coordination.<sup>(13)</sup> Thus, the agglomerated morphology of specimen A, which may have a large fraction of high index planes and a large surface coverage, is superior to the flat morphology. It was shown that the results of specimen A are better than those of specimens B and C in view of the surface area and the number of dissociative adsorption multiplets.

## 5. Conclusions

Thin catalyst films with a large surface area and a high fraction of high index planes were investigated in order to improve the catalytic morphology. In the case of specimen A, the Pt films agglomerated in the form of beads ranging from 100–2,000 Å. In the case of specimen B, the Pt films agglomerated in rectangular shapes with facet features measuring a few micrometers. For specimen C, the Pt films agglomerated in the form of islands measuring a few micrometers. Specimen A, which was fabricated by Pt deposition on Al/SiO<sub>2</sub>/Si followed by thermal oxidation, has better catalyst morphologies than those of specimens B and C with regard to surface area, fraction of high index plane, and the number of dissociative adsorption multiplets. The new catalyst structure, which has an increased number of gas-catalyst reaction multiplets, will contribute to the development of a catalytic micro gas sensor.

## References

- 1 A. R. Baker: UK patent 895230 (1962).
- 2 F. Nuscheler: *Sensors and Actuators* **17** (1989) 593.
- 3 M. Gall: *Sensors and Actuators* **B 4** (1991) 533.
- 4 A. W. van Herwaarden, P. M. Sarro, J. W. Gardner and P. Bataillard: *Digest of Technical Papers 7th International Conference on Solid-State Sensors and Actuators (Transducer '93)* (1993) 411.
- 5 P. Krebs and A. Grisel: *Sensors and Actuators* **B 13** (1993) 555.
- 6 M. Gall: *Sensors and Actuators* **B 15-16** (1993) 260.
- 7 J. H. Visser, M. Zanini, L. Rimai, R. E. Soltis, A. Kovalchuk, D. W. Hoffman, E. M. Logothetis, U. Bonne, L. T. Brewer, O. W. Bynum and M. A. Richard: *The Fifth International Meeting on Chemical Sensors, Technical Digest, Rome 11–14 July (1994)* 468.
- 8 M. Chen and L. D. Schmidt: *J. Catalysis* **55** (1978) 348.
- 9 M. Flytzani-Stephanopoulos, S. Wong and L. D. Schmidt: *J. Catalysis* **49** (1977) 51.
- 10 C. D. Bennewitz, W. D. Westwood and J. D. Brown: *J. Appl. Phys.* **46** (1975) 558.
- 11 W. D. Westwood: *J. Vac. Soc.* **11** (1974) 466.
- 12 I. Barin: *Thermodynamical data of pure substances*, VCH Weinheim (1989).
- 13 G. A. Somorjai and D. W. Blakely: *Nature* **18** (1975) 258.